# Investigation of Tin Liquid Anode on Hybrid Direct Carbon Fuel Cells

Shuangbin L[a], Cairong Jiang[a, b], and John T. S. Irvine[a]
[a] School of Chemistry, University of St Andrews, KY16 9ST, United Kingdom
[b] Department of Materials Science and Engineering, Sichuan University of Science and Engineering, 643000, P. R. China

A novel carbon fuel cell mode was designed for improving the cell performance on hybrid direct carbon fuel cells (HDCFCs). In this paper, the effects of Sn phase as the liquid anode on HDCFCs' performance was investigated. The comparative results indicated that the cell performance was strongly dependent on the amount of Sn loading. With selectivity of different weight ratios, 20 wt% Sn additive was optimized to be the best behavior, corresponding to considerably decreased ohmic and polarization resistance. However, other compositions showed inferior performance than that of Sn-free anode, probably due to the $Li_2SnO_3$ impurity formation impeding catalytic properties of liquid Sn and Li-K salt. Stability testing further implied the cell with 20 wt% Sn addition was the best choice because of maximum fuel efficiency and reasonable durability. Based on these results, the possible completing mechanisms of Sn participating in electrochemical reaction on HDCFCs were proposed.

## Introduction

Compared to boosting the clean energy technology of hydrogen fuels, carbon is much abundant on the earth and is a more conventional energy source for storage and conversion (1, 2). Carbon-fed solid oxide fuel cells, named as direct carbon fuel cells (DCFCs), are alternative energy devices which electrochemically convert chemical energy of solid carbon fuels into electrical energy with high conversion efficiency and less pollution emissions. In spite of these advantages, the confined contact between solid carbon sources and solid electrode /electrolyte interface hinders the active sites for electrochemical oxidation of carbon and thereby limits the cell performance (3). Besides, DCFCs suffer a large activation polarization loss due to the sluggish kinetics of carbon electro-oxidation. As a result, the reformed CO gas via Boudouard reaction at elevated temperatures is preferred to be involved in electrochemical oxidation to improve the power output, whereas decreasing carbon fuel efficiency (4, 5).

The underlying efforts have been to seek ways to extend the reactive areas of solid fuels and the anode. With this motivation, hybrid direct carbon fuel cells (HDCFCs) are considered to be one promising approach of such carbon fuel cells to

overcome this restriction, in which the molten alkali carbonate as carbon transformation carriers in anode chamber of solid oxide fuel cells improves carbon sources diffusion into active sites and thus render a significantly enhanced performance. Jiang (6) reported the direct evidence of the potential configuration with ultrathin YSZ electrolyte achieving the highest power density of 878 $mWcm^{-2}$ at 750 °C to date. More recently, Li (7) verified the outstanding performance using sawdust fuels, which is comparable to hydrogen-fueled carbon fuel cells. Another approach is to introduce a liquid metal (such as Sn) anode on solid oxide electrolyte, favoring carbon electrochemical oxidation via self-redox reaction (8, 9). Such a simplified design eliminates the inevitable corrosion of alkali carbonates on HDCFCs and increases the tolerance of impurities. However, an insulating layer of $SnO_2$ is formed during several hours' testing for liquid metal anode, leading to a performance degradation (10). Taking these factors into consideration, an integration of molten alkali carbonate and liquid Tin metal as the anode components is possible way to achieve excellent performance and stability for applicable purpose. Herein, the incorporation of liquid Sn phase into the anode chamber on HDCFCs was investigated to optimize the cell performance and control the determining parameters on the stability by tuning Sn components.

## Experimental

### Sample preparation and characterization

The commercial graphite flake (Alfa Aesar) was chosen as carbon fuel in this study due to its high carbon purity and stable phase, which is mixed with $Li_2CO_3$ and $K_2CO_3$ composites (62: 38 mol%) at a weight ratio of 1:1. And Sn powders was added into the carbon-carbonate mixture with three compositions of $x$: 1: 1 ($x$ = 0, 0.1, 0.2 and 0.5). To further support the catalytic behaviors of Sn (Aladdin), the 20 wt% $SnO_2$ (Aladdin) was also incorporated into the mixture as comparison. The amount of mixed feedstock was approximately 2 g.

The crystal phases of samples before and after electrochemical testing were characterized by a PANalytical X-ray diffraction equipment (45 kV, 40 mA) using a Cu Kα radiation in the scanning 2θ range of 20-80º. Scanning electron microscopy (SEM) with energy dispersive X-ray spectroscopy (EDX) on a Scios DualBeam Scanning Electron Microscope were conducted to determine the morphology and elemental evolution after testing.

### Cell design and electrochemical measurement

To avoid experimental errors, anode-supported fuel cells were prepared to clearly compare the results of different compositions, consisting of a Ni/ YSZ scaffold (graphite as pore former), a Ni/ YSZ interlayer, a thin YSZ electrolyte (~ 20 μm), a GDC buffer layer and a GDC/LSCF composite cathode. Sliver pastes were bushed onto both electrode sides as current collectors and the prepared button cells were sealed into

lab-built Swagelog jig for electrochemical measurement. The anode chamber was filled with pure $N_2$ of 20 ml/min, and the cathode was exposed to ambient atmosphere. When the system was increased to the operating temperature of 750 °C, the cell performance was carried out on a Solartron 1280b workstation coupled with a 1260 frequency response analyzer using the software Corr-Ware and Z-Plot. The I-V curves were obtained using linear sweep voltammetry at a sweep rate of 20 mV/s from open circuit voltage. The impedance spectra were measured in the frequency that ranged from 0.1 Hz to 1 MHz, and the voltage amplitude was 20 mV. For stability testing, the cell was discharged on potentiostat mode of 0.7 V. A detailed preparation and testing proceedings are described in previous studies (7, 11).

## Results and discussion

To investigate the effects of liquid Sn anode on the HDCFC performance, the I-V and I-P curves of four Ni-YSZ anode supported cells with different Sn contents (0, 10, 20 and 50 wt%) were measured at 750 °C, as shown in Figure 1. For Sn-free anode, the peak power density exhibited about 65 mW $cm^{-2}$, which is much smaller than previously reported by the anode supported cells of carbon black pore former due to insufficient gas pathways in anode structure (11). When introducing Sn phase into anode, the OCV (open circuit voltage) doesn't change significantly, indicating the OCV is still dominated by the co-effects of carbon and carbonates other than liquid Sn phase. Whereas the incorporation of Sn reflects variant peak power densities, strongly dependent on the Sn concentrations. The values of which are 58, 86 and 49 mW $cm^{-2}$ for 10, 20 and 50 wt% loading, respectively. It should be noted that the addition of liquid Sn couldn't improve the nonlinear I-V curves induced by sluggish kinetics of graphite carbon oxidation. That means despite the remarkable improvement of performance in 20 wt% Sn loading on HDCFCs, the limitation of solid carbon and anode interface still impedes the electrochemical process.

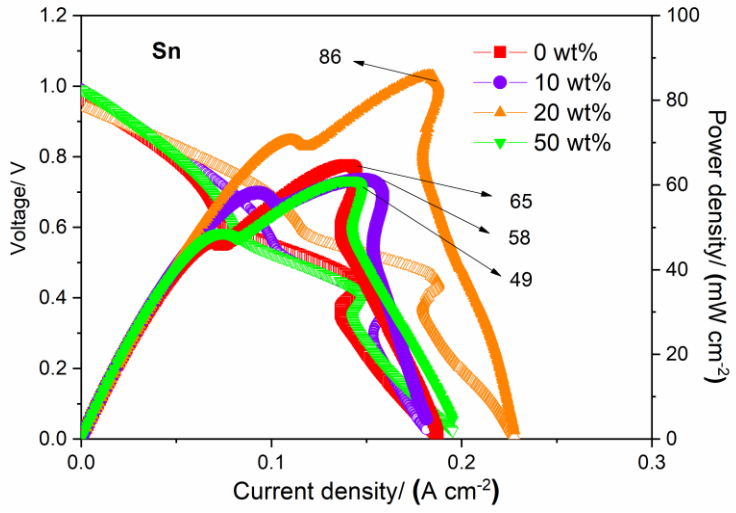


Figure 1. I-V and I-P curves with different Sn contents measured at 750 °C.

The electrochemical impedance spectra of corresponding compositions measured at 750 °C were shown in Figure 2, consistent with the results observed from I-V curves. Obviously, the 20 wt% Sn loading with best cell performance showed the lowest ohmic and polarization resistance. It also can be could that all impedance spectra consisted of higher, medium and lower-frequency arcs. Generally, the higher and medium frequency region is mainly related to the charge transfer process including surface oxygen exchange kinetics at cathode side and catalytic electro-oxidation reactions at anode side. We neglected the polarization contribution from the cathode due to its higher oxygen exchange activity of LSCF. That is, the chemical and electrochemical equilibriums at the anode dominate the charge transfer loss. While the lower frequency arc is ascribed to gas adsorption/ desorption and diffusion process (12). From the point of view, the superior performance for 20 wt% Sn is an optimal convergence towards variant compositions, enabling remarkably reduced ohmic and polarization resistance that are probably driven by the multiple reaction mechanisms.

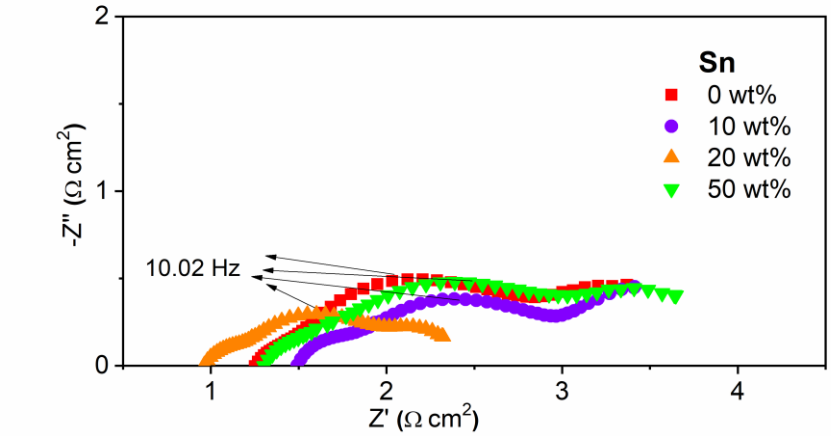


Figure 2. Corresponding impedance spectra with different Sn contents measured at OCV condition.

During fuel cell operation, for example, the liquid Sn not only acts as a good electronic conductor, favoring electronic current dispersion across the entire anode, but also catalyzes carbon oxidation via self-redox cycling, as described in Eq.1 and 2.

$$Sn + 2O^{2-} \rightarrow SnO_2 + 4e^- \quad [1]$$

$$C + SnO_2 \rightarrow Sn + CO_2 \quad [2]$$

Unfortunately, the melting point of oxidation product ($SnO_2$) is 1630 °C, far exceeding the operating temperature with respective to Sn metal (232 °C). In this case, an insulating $SnO_2$ might be deposited at the catalytically reactive interface, leading the performance degradation. On the other hand, the Li-K molten salt is demonstrated to be a good ionic conductor, being able to overcome sluggish carbon oxidation by releasing $O^{2-}$ and regenerating $CO_3^{2-}$ with the chemical equilibrium of Eq. 3 (13).

Furthermore, $CO_3^{2-}$ is considered as the carbon carrier facilitating the carbon electro-oxidation via Eq. 4. Combined with catalytic properties of liquid Sn phase and Li-K carbonate that can extend the reactive region to three dimensions, the introduction of Sn into the HDCFCs should be supposed to favor the cell performance independent of Sn contents. However, other compositions show inferior performance exception of 20 wt% Sn, shown in Fig. 1.

$$CO_3^{2-} \leftrightarrow CO_2 + O^{2-} \quad [3]$$

$$C + 2CO_3^{2-} \rightarrow 3CO_2 + 4e^- \quad [4]$$

**TABLE I.** Calculated mass changes of compositions in feedstocks.

| Initial mass of Sn (g) | Mass loss of Sn (g) | Mass loss of $Li_2CO_3$ (g) |
|---|---|---|
| 0 (0 wt%) | 0 | 0.37 |
| 0.08 (10 wt%) | 0.08 | 0.05 |
| 0.16 (20 wt%) | 0.16 | 0.1 |
| 0.40 (50 wt%) | 0.40 | 0.25 |

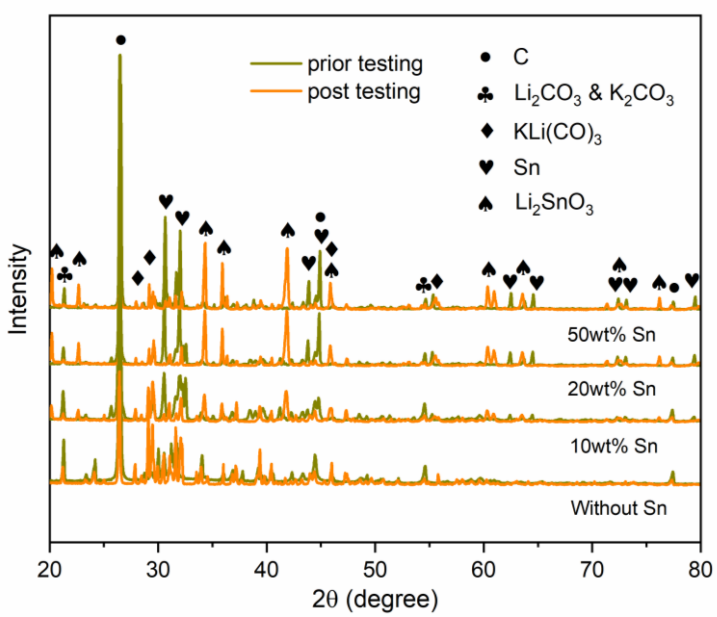


Figure 3. XRD patterns of Sn-carbon-carbonate mixture prior- and post-testing.

To determine unfavorable effects on multiple reaction mechanisms, the XRD patterns of Sn-carbon-carbonate mixture prior- and post-testing were compared in Figure 3. For free Sn, clusters of peaks around 29° observed after testing were corresponding to characteristic peaks of $KLi(CO_3)$ phase, which is considered to be the existing state of Li-K eutectic salt. With increasing the loading of Sn, the intensity of $KLi(CO_3)$ phase was decreased, coupled with completely disappeared Sn phase after

testing. Unfortunately, undesired phase of $Li_2SnO_3$ impurity was detected in the patterns and the amount was increased with Sn increasing. We thus conclude that the formation of $Li_2SnO_3$ impurity may be the incentive for a drop performance of Sn-incorporated HDCFCs via a typical high temperature solid state reaction (Eq. 5). In this reaction, $Li_2CO_3$ component extracted from $KLi(CO_3)$ phase is likely to react with $SnO_2$ from Eq.1, competing with catalytic loop process involved in Sn redox cycling (Eq.1 and 2) and chemical equilibrium of $CO_3^{2-}$ (Eq.3 and 4). As a result, such three interactional reactions probably control over the capability of electrochemical carbon oxidation, as depicted in Fig. 4. Another indirect evidence was that the excessive mass of $Li_2CO_3$ to Sn in Eq. 5 supports competing reaction mechanisms, as calculated in Table 1. For lower amounts of Sn (10 wt%), the relatively low catalytic properties of cycle of Sn redox reaction can partially inhibit the exceedingly catalytic properties of Li-K salt, thus degrading the performance moderately (Figure1). If the concentration of Sn is enough (50 wt%) close to that of $Li_2CO_3$, the catalytic behavior of Li-K salt is neglected since most $Li_2CO_3$ is converted to $Li_2SnO_3$ phase, resulting highly lower performance. When tuning the Sn ratio to an optimal level (20 wt%), the catalytic reactions of both Sn-$SnO_2$ and Li-K systems exert a great electrochemical performance, as well as the least disruptive impact of $Li_2SnO_3$ impurity.

$$Li_2CO_3 + Sn + O_2 \rightarrow Li_2SnO_3 + CO_2 \quad [5]$$

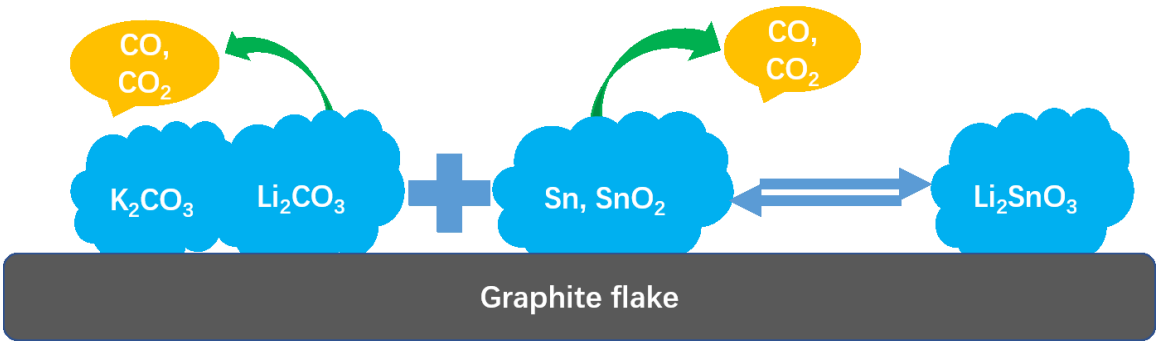


Figure 4. Possible reaction schemes of liquid Sn anode on HDCFCs.

Afterwards, we also investigated the electrochemical behaviors for 20 wt% $SnO_2$ additive on HDCFCs at 750 °C, shown in Figure 5. A peak power density observed was 73 mW $cm^{-2}$, lower than that observed with 20 wt% Sn additive. The performance improvement is probably originated from decentralized Sn-$SnO_2$ cycling and the increase of $CO_2$ concentration from Eq. 5, leading to the decreased polarization resistance in EIS spectra. Unlike solid $SnO_2$ (Figure 2), the liquid Sn phase not only could improve the contact resistance of solid carbon and anode, thus increasing active sites of carbon oxidation. But also remarkably reduce the polarization resistance from charge transfer and gas diffusion.

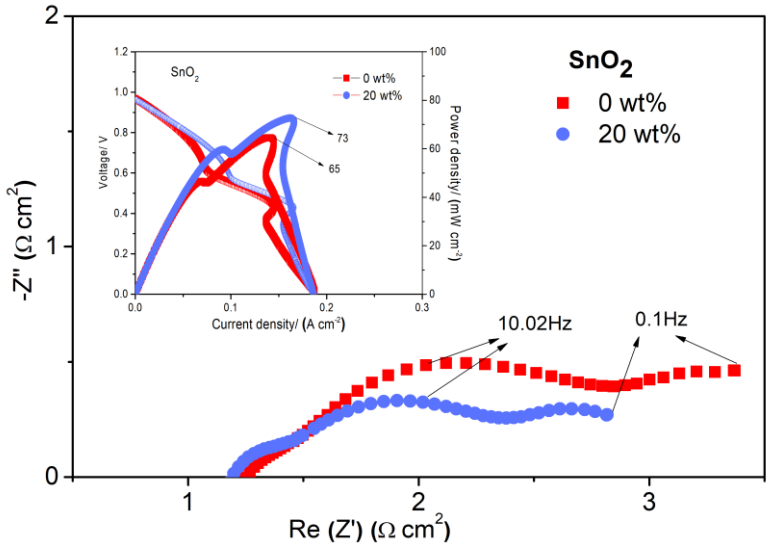


Figure 5. V-I-P curves and EIS spectra of $SnO_2$-containing HDCFCs measured at 750 °C.

Durabilities for Sn- and $SnO_2$-containing HDCFCs were performed until the cells died at a constant voltage of 0.7 V and 750 °C, shown in Figure 6. The lifetime of free Sn and $SnO_2$ additives was 40.7 h, exhibiting continuous degradation during discharging period. But for the cells with Sn and $SnO_2$ additives, the degrading process seemed to be considered as two relatively steady stages, especially for 10 wt% Sn and 20 wt% $SnO_2$. The cell with 50 wt% Sn was an exception due to most of $Li_2CO_3$ compositions are consumed to $Li_2SnO_3$ phase during discharging operation. Obviously, the lifetime for observed results is in following sequence: 10 wt% Sn > 0 wt% Sn > 50 wt% Sn > 20 wt% Sn > 20 wt% $SnO_2$. In order to further understand liquid Sn anode on HDCFCs, fuel utilization efficiencies were calculated using Eq. 6:

$$\eta = \frac{n_{electricity}}{n_{total}} \times 100\% = \frac{It/zF}{m/M} \times 100\% \qquad [6]$$

This equation is based on the assumption that Faraday efficiency is unit. Where $I$ is the current, $t$ is the testing time, $m$ and $M$ are the mass and mole mass of carbon, respectively, $F$ is the Faraday constant and $z$ corresponds to the electron transfer number. According to Eq.6, we assumed the electrochemical oxidation of carbon is complete, indication of z = 4. The summarized results of fuel efficiencies in Figure 6 implied the concentration of 20 wt% Sn addition with the maximum efficiency of 46.69 % is the promising candidate for improved performance on HDCFCs, considering the results of durability and power density. In spite of better electrochemical behavior for 20 wt% $SnO_2$, the reduced lifetime and lower carbon utilization efficiency demonstrate that the immobile solid $SnO_2$ phase cannot form consecutive network, replacing the role of fluid liquid Sn under operating conditions.

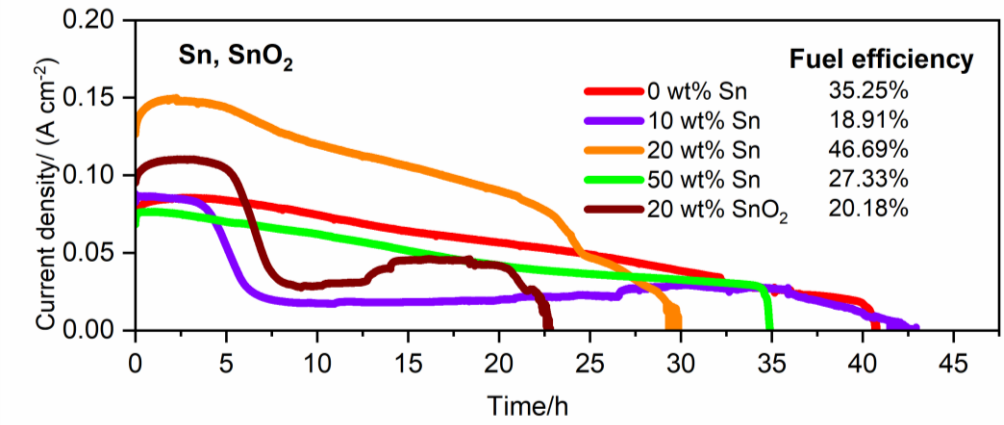


Figure 6. Durability measurements for Sn- and $SnO_2$-containing HDCFCs at a constant voltage of 0.7 V and 750 °C.

The effects of liquid Sn phase on the microstructure and element distribution across the anode scaffold were evaluated after durability testing, as presented in Figure 7. During long operating period, small carbon particles just like flakes (green region) accumulated in fuel gas channels, thus impairing gas diffusion pathways and blocking the active sites. As a result, such carbon deposition observations lead to a continuous performance degradation. In addition, more Sn incorporation seemed to alleviate carbon accumulation, but resulted in more undesired $Li_2SnO_3$ impurity formation. It should be noted that after testing, Sn-containing phases were absent within the entire anode structure from EDX results, indicating that almost Sn exists on the anode surface probably to participate in catalytic reaction and form $Li_2SnO_3$ impurity.

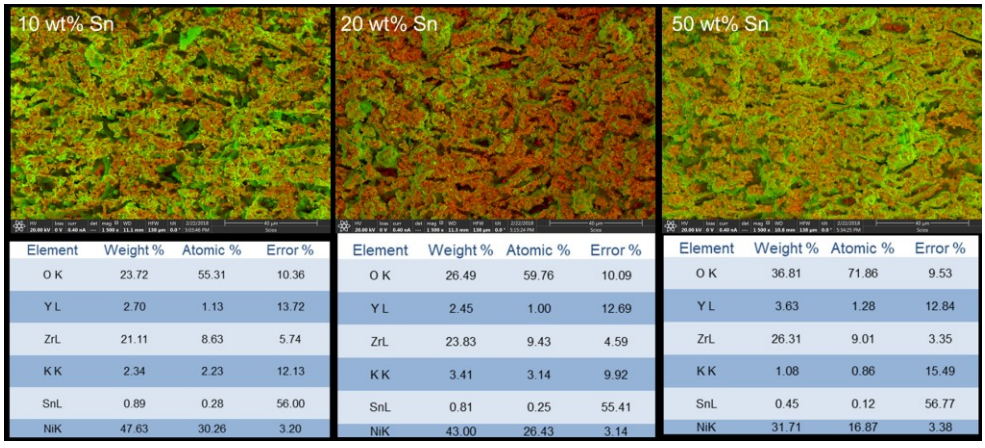


| Element | Weight % | Atomic % | Error % |
|---|---|---|---|
| O K | 23.72 | 55.31 | 10.36 |
| Y L | 2.70 | 1.13 | 13.72 |
| Zr L | 21.11 | 8.63 | 5.74 |
| K K | 2.34 | 2.23 | 12.13 |
| Sn L | 0.89 | 0.28 | 56.00 |
| Ni K | 47.63 | 30.26 | 3.20 |

| Element | Weight % | Atomic % | Error % |
|---|---|---|---|
| O K | 26.49 | 59.76 | 10.09 |
| Y L | 2.45 | 1.00 | 12.69 |
| Zr L | 23.83 | 9.43 | 4.59 |
| K K | 3.41 | 3.14 | 9.92 |
| Sn L | 0.81 | 0.25 | 55.41 |
| Ni K | 43.00 | 26.43 | 3.14 |

| Element | Weight % | Atomic % | Error % |
|---|---|---|---|
| O K | 36.81 | 71.86 | 9.53 |
| Y L | 3.63 | 1.28 | 12.84 |
| Zr L | 26.31 | 9.01 | 3.35 |
| K K | 1.08 | 0.86 | 15.49 |
| Sn L | 0.45 | 0.12 | 56.77 |
| Ni K | 31.71 | 16.87 | 3.38 |

Figure 7. The cross-sectional microstructure and EDX results of liquid Sn anode after durability testing.

## Conclusion

In this study, initial electrochemical performance measurements were performed to verify the possibility of liquid Sn anode on HDCFCs. With introducing the increased Sn content, the OCV was still influenced by carbon and carbonates mixture due to low

Sn concentration. Whereas only 20 wt% Sn incorporation showed the superior performance than that of free-Sn anode with remarkably reduced ohmic and polarization resistance. Such kinetics of electrochemical oxidation of carbon probably can be controlled by three competing reaction mechanisms: Sn redox reaction, chemical equilibrium of Li-K salt and unfavorable $Li_2SnO_3$ formation. In contrast to Sn, the improved performance of 20 wt% $SnO_2$ almost resulted from reduced polarization resistance because of immobile state. Considering the results of electrochemical behaviors, fuel efficiency and durability, the 20 wt% Sn addition into anode is a promising approach to enhance the performance in spite of $Li_2SnO_3$ impurity formation.

## Acknowledgments

S.B. acknowledges the financial support of China Scholarship Council (CSC). C.J. acknowledges the Royal Society of Edinburgh for an RSE BP Hutton Prize in Energy Innovation. The authors also acknowledge Jianing Hui for FEI Scios measurement.

## References

1. H.J. Li, Q.H. Liu, Y.D. Li, *Electrochimica Acta*, **55**, 1958 (2010).
2. L.W. Chen, H.C. Zhang, S.H. Gao, *Int. J. Electrochem. Sc.*, **9**, 5788 (2014).
3. M. Konsolakis, N. Kaklidis, G.E. Marnellos, D. Zaharaki, K. Komnitsas, *Rsc Advances*, **5**, 73399 (2015).
4. A.C. Lee, S. Li, R.E. Mitchell, T.M. Guer, *Electrochem. Solid. St.*, **11**, B20 (2008).
5. A.C. Rady, S. Giddey, A. Kulkarni, S.P.S. Badwal, S. Bhattacharya, *Electrochimica Acta*, **143**, 278 (2014).
6. C.R.M. Jiang, J. J. Bonaccorso, A. D. Irvine, J. T. S., *Energ. Environ. Sci.*, **5**, 6973 (2012).
7. S. Li, C. Jiang, J. Liu, H. Tao, X. Meng, P. Connor, J. Hui, S. Wang, J. Ma, J.T.S. Irvine, *J. Power Sources*, **383**, 10 (2018).
8. H. Ju, S. Uhm, J.W. Kim, R.-H. Song, H. Choi, S.-H. Lee, J. Lee, *J. Power Sources*, **198**, 36 (2012).
9. H. Wang, Y. Shi, N. Cai, *Int. J. Hydrogen Energ.*, **38**, 15379 (2013).
10. H. Wang, Y. Shi, W. Yuan, T. Cao, N. Cai, X. Liang, *ECS Transactions*, **57**, 2913 (2013).
11. S.B. Li, W.Z. Pan, S.R. Wang, X. Meng, C.R. Jiang, J.T.S. Irvine, *Int. J. Hydrogen Energ.*, **42**, 16279 (2017).
12. Y. Zhou, C. Yuan, T. Chen, X. Meng, X. Ye, J. Li, S. Wang, Z. Zhan, *J. Power Sources*, **267**, 117 (2014).
13. Y. Nabae, K.D. Pointon, J.T.S. Irvine, *Energ. Environ. Sci.*, **1**, 148 (2008).